The Astrophysical Journal, 591:288–300, 2003 July 1

HOW MASSIVE SINGLE STARS END THEIR LIFE

A. Heger[1]
Department of Astronomy and Astrophysics, Enrico Fermi Institute, University of Chicago, 5640 South Ellis Avenue, Chicago, IL 60637; 1@2sn.org

C. L. Fryer
Theoretical Astrophysics, MS B288, Los Alamos National Laboratories, Los Alamos, NM 87545; fryer@lanl.gov

S. E. Woosley
Department of Astronomy and Astrophysics, University of California, Santa Cruz, CA 95064; woosley@ucolick.org

N. Langer
Astronomical Institute, P.O. Box 80000, NL-3508 TA Utrecht, Netherlands; n.langer@astro.uu.nl

and

D. H. Hartmann
Department of Physics and Astronomy, Clemson University, Clemson, SC 29634-0978; hdieter@clemson.edu
Received 2002 December 19; accepted 2003 March 11

ABSTRACT

How massive stars die—what sort of explosion and remnant each produces—depends chiefly on the masses of their helium cores and hydrogen envelopes at death. For single stars, stellar winds are the only means of mass loss, and these are a function of the metallicity of the star. We discuss how metallicity, and a simplified prescription for its effect on mass loss, affects the evolution and final fate of massive stars. We map, as a function of mass and metallicity, where black holes and neutron stars are likely to form and where different types of supernovae are produced. Integrating over an initial mass function, we derive the relative populations as a function of metallicity. Provided that single stars rotate rapidly enough at death, we speculate on stellar populations that might produce gamma-ray bursts and jet-driven supernovae.

Subject headings: black hole physics — gamma rays: bursts — stars: early-type — stars: neutron — supernovae: general

1. INTRODUCTION

The fate of a massive star is governed chiefly by its mass and composition at birth and by the history of its mass loss. For single stars, mass loss occurs as a result of stellar winds, for which there exist semiempirical estimates. Thus, within currently existing paradigms for the explosion, the fate of a star of given initial mass and composition is determined (the Russell-Vogt theorem). If so, one can calculate realization frequencies for stellar explosions and remnants of various kinds and estimate how these might have evolved with time.

Such estimates are fraught with uncertainty. The litany of complications is long and requires discussion (§ 6). No two groups presently agree, in detail, on the final evolution of *any* massive star (including its explosion energy, remnant mass, and rotation rate), and the scaling of mass loss with metallicity during different evolutionary stages is widely debated. Still, it is worthwhile to attempt an approximate table of histories. We would like to know, within the comparatively well understood domain of stars that do not experience mass exchange with a companion and for a particular set of assumptions regarding mass loss and explosion, what sort of supernova (SN) each star produces and what sort of bound remnant, if any, it leaves. If possible, we would also like some indication of which massive stars might make gamma-ray bursts.

In this paper we construct such a table of stellar fates and remnants. In § 2 we describe our assumptions regarding mass loss and explosion mechanism(s) and in § 3 the remnant properties, and in § 6 we discuss the uncertainties. Section 4 delineates the sorts of stellar explosions and collapses we want to distinguish, and in § 5 we discuss the resulting realizations of different outcomes as a function of metallicity in the galaxy.

2. ASSUMPTIONS

2.1. *Stellar Models and Paradigms*

The stellar models used in this paper were taken from Woosley & Weaver (1995), Heger & Woosley (2002), Woosley, Heger, & Wheeler (2002), and A. Heger, S. E. Woosley, & R. D. Hoffman (2003 in preparation). These papers treat the evolution of massive stars in the range 9–300 $M_{\odot}$, calculated without rotation from birth on the main sequence to death, as either iron core-collapse supernovae (helium core masses at death less than $\sim$65 $M_{\odot}$) or pair-instability supernovae (helium core masses at death greater than $\sim$65 $M_{\odot}$ and up to about 135 $M_{\odot}$). The effects of mass loss were included in those studies, as discussed in § 2.2.

We presume here that the explosion mechanism, however it may operate, and the remnant properties are determined

[1] Current address: Theoretical Astrophysics Group, MS B227, Los Alamos National Laboratory, Los Alamos, NM 87545.

by the mass of the helium core when the star dies. (Perhaps the carbon oxygen core mass is a better discriminant, but systematics of the two are very similar.) As the mass of the helium core increases, so does its binding energy and entropy. Because of its higher entropy, a larger helium core also has, on the average, a larger iron core mass and a shallower density gradient around that core (Woosley et al. 2002). Consequently, such stars are harder to explode (Fryer 1999; Fryer & Kalogera 2001). Even in "successful" explosions, where a strong outward shock is born, mass may later fall back onto a neutron star remnant, turning it, within seconds to tens of hours, into a black hole (BH). We thus distinguish black holes that are produced promptly or "directly" from those made by fallback.

Fryer (1999) has estimated that the helium core mass where black hole formation by fallback ensues is about 8 $M_\odot$ (a $\lesssim$25 $M_\odot$ main-sequence star) and that direct black hole formation occurs for helium cores over 15 $M_\odot$ (a 40 $M_\odot$ main-sequence star with no mass loss). These numbers are uncertain (§ 6.2), but are representative choices. It is assumed that a baryonic remnant mass of over 2.0 $M_\odot$ will produce a black hole.

While the helium core mass governs the explosion mechanism, the hydrogen envelope is largely responsible for determining the spectrum (at peak) and light curve of common Type II supernovae. Stars having massive hydrogen envelopes when they die will be Type IIp; low-mass envelopes will give Types IIL and IIb, etc. (§ 4). An exception are supernovae of Types Ib and Ic, whose light curves do depend sensitively on the helium core mass since all the hydrogen envelope has been removed. The light curves of Types IIb, Ib, Ic, and 87A-like explosions are also sensitive to the amount of ^{56}Ni made in the explosion.

2.2. *Mass Loss*

The principal physics connecting the final evolution of a star to its metallicity is its mass loss. Low-metallicity stars have less mass loss and bigger helium cores and hydrogen envelopes when they die. To a lesser extent, metallicity also affects whether the presupernova star is a red or blue supergiant (Langer & Maeder 1995).

For main-sequence stars and red supergiants, the mass-loss rates employed in the studies cited above were taken from Nieuwenhuijzen & de Jager (1990). For Wolf-Rayet stars, a mass-dependent mass-loss rate (Langer 1989) was assumed using the scaling law established by Brown (1997) and Wellstein & Langer (1999), but lowered by a factor of 3 (Hamann & Koesterke 1998). Wind-driven mass loss is believed to be metallicity-dependent, and a scaling law $\propto\sqrt{Z}$ has been suggested for hot stars (Kudritzki 2000; Nugis & Lamers 2000). Woosley et al. (2002) assumed that the same scaling law holds for Wolf-Rayet stars (Vanbeveren 2001) and blue and red supergiants as well. "Metallicity" is assumed here to be the initial abundance of heavy elements, especially of iron, and not the abundances of new heavy elements, like carbon and oxygen, in the atmospheres of WC and WO stars (§ 6.1).

In very massive stars above $\sim$60 $M_\odot$, the ϵ-mechanism for pulsational driven mass loss sets in and enhances the mass loss during central hydrogen burning. Opacity-driven pulsations also become important, if not dominant, at high metallicity (Baraffe, Heger, & Woosley 2001). At very low metallicity, on the other hand, Baraffe et al. (2001) have shown that primordial stars should not have significant mass loss due to pulsations. This suggests significant evolution in the mass loss of very massive stars with metallicity (Figs. 1–4).

3. REMNANT PROPERTIES

Figure 1 shows the expected remnant types as a function of mass and initial "metallicity" for the above assumptions. In preparing Figure 1, it is assumed that stars below $\sim$9 $M_\odot$ do not form massive enough cores to collapse—that they end their lives as white dwarfs. Just above this mass lies a narrow range, $\sim$9–10 $M_\odot$, where degenerate oxygen-neon cores are formed that either collapse because of electron capture (Barkat, Reiss, & Rakavy 1974; Miyaji et al. 1980; Nomoto 1984; Habets 1986; Miyaji & Nomoto 1987; Nomoto 1987; Nomoto & Hashimoto 1988) and make a neutron star or lose their envelopes and make white dwarfs (Garcia-Berro & Iben 1994; Ritossa, Garcia-Berro, & Iben 1996; Garcia-Berro, Ritossa, & Iben 1997; Iben, Ritossa, & Garcia-Berro 1997; Ritossa, Garcia-Berro, & Iben 1999). Above $\sim$10 $M_\odot$ core collapse is the only alternative.

Wherever this transition between white dwarf formation and iron core collapse lies, it should depend very little on metallicity and thus appears as a vertical line in Figure 1. At low metallicities, the boundaries for black hole formation are also defined entirely by the initial stellar mass since there is a one-to-one correspondence between initial stellar mass and final helium core mass.

For stars of higher metallicity, mass loss becomes increasingly important, resulting in smaller helium cores for a given initial mass. If the star loses its entire hydrogen envelope (to the right of the green line in Figs. 1–4), its rate of mass loss increases significantly (see, e.g., Langer 1989; Hamann, Koesterke, & Wessolowski 1995), producing much smaller helium cores at collapse. This effect underlies the abrupt change in the otherwise vertical boundaries between neutron star, fallback black hole, and direct black hole formation. For very massive stars, the remnant of the collapsing star depends sensitively on the metallicity. Above 40 $M_\odot$, low-metallicity stars form black holes directly, while at higher metallicities, black holes of smaller mass are produced by fallback until, ultimately, only neutron stars are made. Winds are assumed to be stronger in higher mass stars, so the metallicity at which these transitions occur decreases with mass. But beyond $\sim$100 $M_\odot$, this limit may rise again because of high enough initial mass or the significant role of evolution phases with lower mass-loss rates (e.g., a WNL phase; see Brown et al. 2001).

At low metallicities, there is also a range of masses for massive stars that leave behind no remnant whatsoever. These are the pair-instability supernovae. If the helium core exceeds $\sim$65 $M_\odot$, corresponding to a $\sim$140 $M_\odot$ initial mass for stars without mass loss, the pulsational pair instability (Heger & Woosley 2002) becomes so violent that the star is disrupted entirely. When the helium core mass at the end of central carbon burning exceeds $\sim$135 $M_\odot$ for nonrotating stars (initial mass of $\sim$260 $M_\odot$ without mass loss), photodisintegration in the center leads to collapse to a very massive black hole ($\gtrsim$100 $M_\odot$), once again forming a black hole directly (Fryer, Woosley, & Heger 2001; Heger & Woosley 2002). However, as the metallicity increases, mass loss shifts the regime of pair-instability supernovae to higher initial masses. At still higher metallicities, these supernovae do not

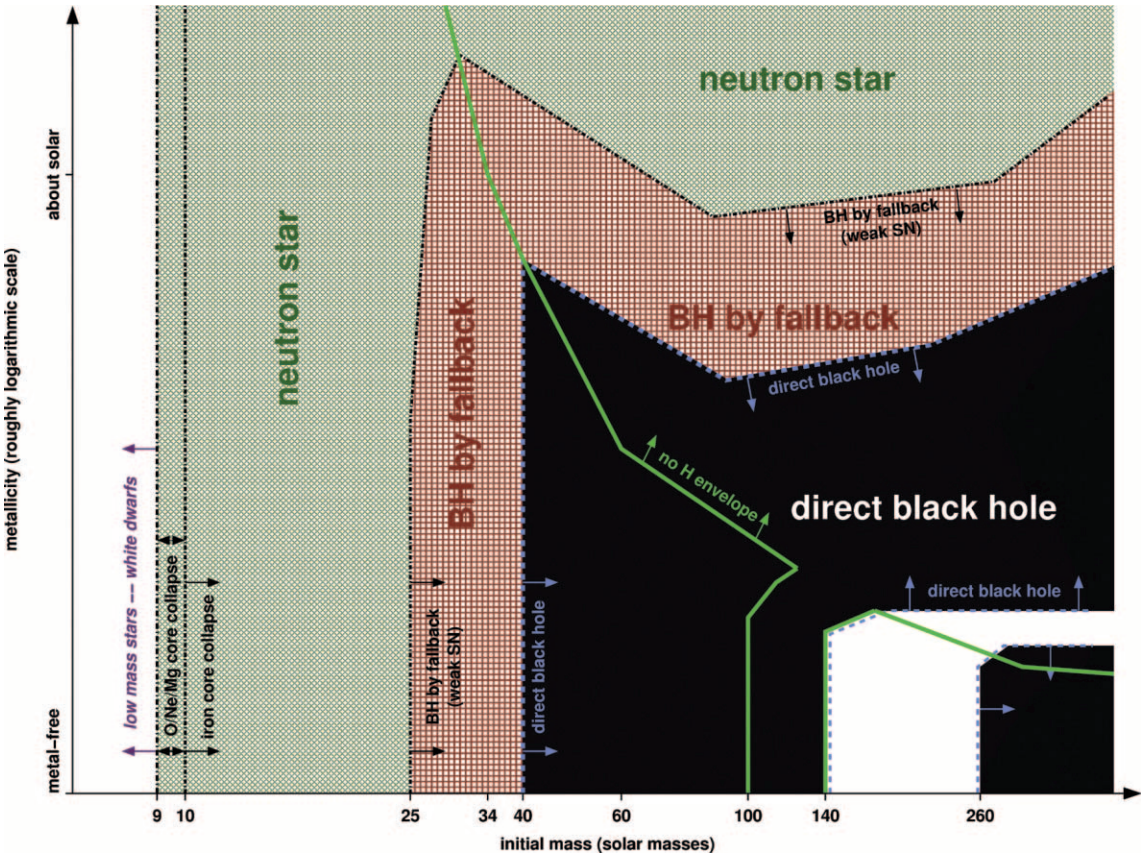

FIG. 1.—Remnants of massive single stars as a function of initial metallicity (*y-axis*; qualitatively) and initial mass (*x-axis*). The thick green line separates the regimes where the stars keep their hydrogen envelope (left and lower right) from those where the hydrogen envelope is lost (upper right and small strip at the bottom between 100 and 140 $M_{\odot}$). The dashed blue line indicates the border of the regime of direct black hole formation (*black*). This domain is interrupted by a strip of pair-instability supernovae that leave no remnant (*white*). Outside the direct black hole regime, at lower mass and higher metallicity, follows the regime of BH formation by fallback (*red cross-hatching and bordered by a black dot-dashed line*). Outside of this, green cross-hatching indicates the formation of neutron stars. The lowest mass neutron stars may be made by O/Ne/Mg core collapse instead of iron core collapse (*vertical dot-dashed lines at the left*). At even lower mass, the cores do not collapse and only white dwarfs are made (*white strip at the very left*).

occur at all (Baraffe et al. 2001) because the progenitor stars are pulsationally unstable.

4. SUPERNOVAE

4.1. *Supernovae of Type IIp and IIL*

It has long been recognized that massive stars produce supernovae (Baade & Zwicky 1934). In this paper, we assume the progenitor properties for the different core-collapse supernova types listed in Table 1.

The lower and upper limits of main-sequence mass that will produce a successful supernova ("*M*-lower" and "*M*-upper")—one with a strong outgoing shock still intact at the surface of the star—have long been debated. On the lower end, the limit is set by the heaviest star that will eject its envelope quiescently and produce a white dwarf. Estimates range from 6 to 11 $M_{\odot}$, with smaller values characteristic of calculations that are employed using a large amount of convective overshoot mixing (Marigo, Bressan, & Chiosi 1996; Chiosi 2000) and the upper limit determined by whether helium shell flashes can eject the envelope surrounding a neon-oxygen core in the same way they do for carbon-oxygen cores (§ 3). It may also slightly depend on metallicity (Cassisi & Castellani 1993). Here we will adopt 9 $M_{\odot}$ for *M*-lower.

TABLE 1
PROGENITOR PROPERTIES FOR DIFFERENT CORE-COLLAPSE SUPERNOVAE

SN Type	Pre-SN Stellar Structure
IIp.....	$\gtrsim 2\ M_{\odot}$ H envelope
IIL/b	$\lesssim 2\ M_{\odot}$ H envelope
Ib/c.....	No H envelope

The value of *M*-upper depends on details of the explosion mechanism and is even more uncertain (§ 6.2). Fryer & Kalogera (2001) estimate 40 $M_{\odot}$, but calculations of explosions even in supernovae as light as 15 $M_{\odot}$ give widely varying results. It is likely that stars up to at least 25 $M_{\odot}$ do explode, by one means or another, in order that the heavy elements are produced in solar proportions. The number of stars between 25 and 40 $M_{\odot}$ is not large. Here we have taken what some may regard as a rather large value: *M*-upper = 40 $M_{\odot}$ (Fig. 2).

For increasing metallicity, mass loss reduces the hydrogen envelope at the time of core collapse. A small hydrogen envelope ($\lesssim 2\ M_{\odot}$) cannot sustain a long plateau phase in the light curve, and only Type IIL/b supernovae or, for very thin hydrogen layers, Type IIb supernovae result (Barbon, Ciatti, & Rosino 1979; Filippenko 1997). It is also necessary

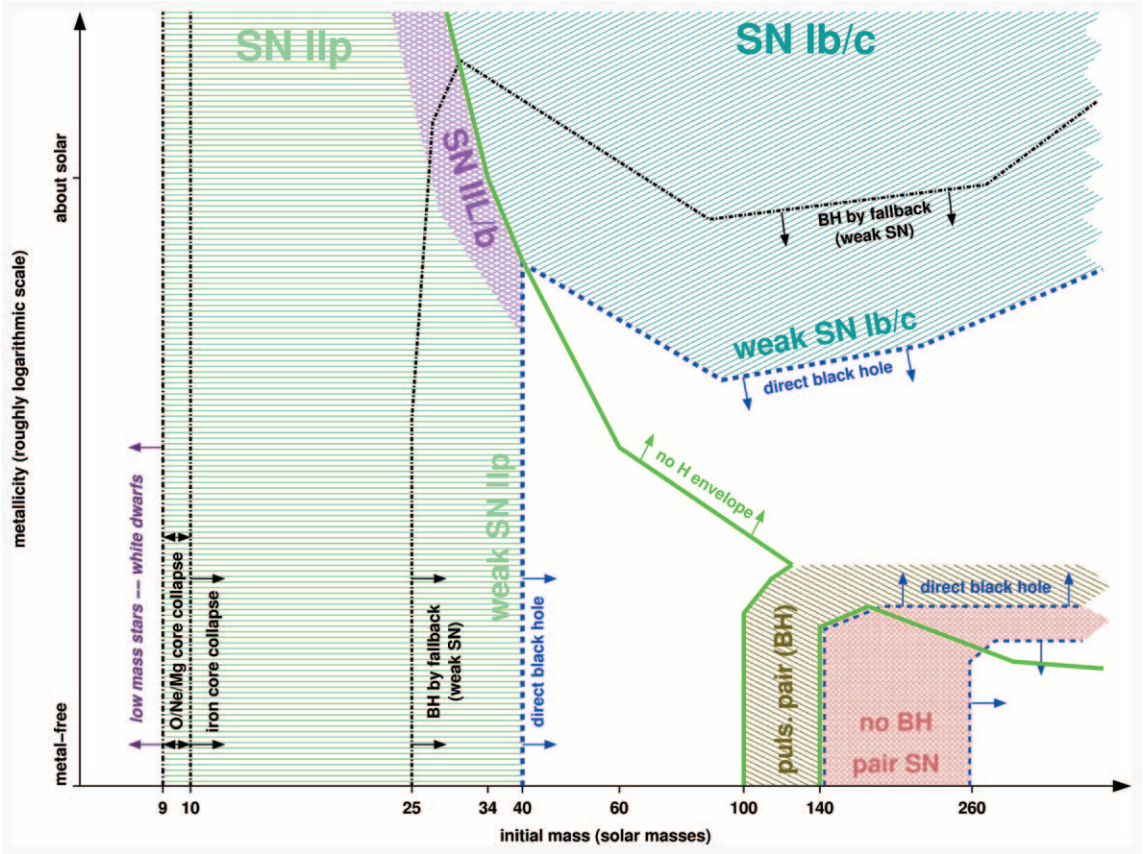

FIG. 2.—Supernovae types of nonrotating massive single stars as a function of initial metallicity and initial mass. The lines have the same meaning as in Fig. 1. Green horizontal hatching indicates the domain where Type IIp supernovae occur. At the high-mass end of the regime they may be weak and observationally faint because of fallback of ^{56}Ni. These weak SN Type IIp should preferentially occur at low metallicity. At the upper right-hand edge of the SN Type II regime, close to the green line of loss of the hydrogen envelope, Type IIL/b supernovae that have a hydrogen envelope of $\lesssim 2\ M_{\odot}$ are made (*purple cross-hatching*). In the upper right-hand quarter of the figure, above both the lines of hydrogen envelope loss and direct black hole formation, Type Ib/c supernovae occur; in the lower part of their regime (middle of the right half of the figure) they may be weak and observationally faint because of fallback of ^{56}Ni, similar to the weak Type IIp SNe. In the direct black hole regime no "normal" (non–jet-powered) supernovae occur since no SN shock is launched. An exception are pulsational pair-instability supernovae (lower right-hand corner; *brown diagonal hatching*) that launch their ejection before the core collapses. Below and to the right of this we find the (nonpulsational) pair-instability supernovae (*red cross-hatching*), making no remnant, and finally another domain where black hole are formed promptly at the lowest metallicities and highest masses (*white*) where nor SNe are made. White dwarfs also do not make supernovae (*white strip at the very left*).

for Type IIL supernovae that the radius be large (Swartz, Wheeler, & Harkness 1991) and helpful if the ^{56}Ni mass is not too small. The minimum metallicity for Type IIL/b supernovae in single stars is set by the requirement that the mass loss needs to be strong enough to remove enough of the hydrogen envelope (Fig. 2). In single stars Type IIL/b SNe are formed only in a thin strip where the hydrogen envelope is almost, but not entirely, lost. Gaskell (1992) finds that Type IIL supernovae are currently about 10%–20% as frequent as Type IIp.

For increasing metallicity, this domain shifts to lower initial mass. Below a certain minimum metallicity we do not expect Type IIL/b supernovae from single stars at all. Indeed, those stars that form at the lowest (possible) metallicities will be so massive that they frequently form black holes by fallback and have not very luminous supernovae. This will be particularly true if the stars explode as blue supergiants but lack radioactivity.

4.2. *Type Ib and Ic Supernovae*

A complication is that Type Ib/c SNe with masses above 4–5 $M_{\odot}$, which may be the most common ones to come from single stars, also have dim displays even if they are still powerful explosions (Ensman & Woosley 1988); i.e., the progenitor stars' cores are not so massive that they encounter significant fallback. In this paper, we do not differentiate these types of supernovae from our set of normal supernovae. Our assumptions regarding the different types of supernovae are summarized in Table 2.

Clearly, mass loss is a key parameter, and both high metallicities and high initial masses are required to produce

TABLE 2
EXPLOSION ASSUMPTIONS FOR DIFFERENT SUPERNOVA TYPES

Type Ib/c He Core Mass at Explosion ($M_{\odot}$)	Explosion Energy	Display
$\gtrsim 15$	Direct collapse	None[a]
~ 15–8	Weak	Dim[a]
~ 8–5	Strong	Possibly dim
$\lesssim 5$	Strong	Bright

[a] If not rotating.

Type Ib/c supernovae in single stars. Woosley et al. (2002) find that for solar metallicity, the limit for nonrotating stars is $\sim$34 $M_\odot$. These supernovae can be weak, and their later fallback will produce BH remnants. As with the Type II black hole–forming supernovae, we anticipate that this fallback, in particular of the ^{56}Ni lost this way, may weaken the brightness of the supernova display, similar to the case of weak Type II SNe.

4.3. *Nickel-deficient Supernovae*

The light curve of most supernovae is a consequence of two energy sources—shock-deposited energy and radioactivity, especially the decay of ^{56}Ni to ^{56}Fe. There are cases, however, in which the radioactive component may be weak or absent. If the hydrogen envelope is still present, a bright supernova may still result, with the brightness depending on the explosion energy (Popov 1993), but the light curve lacks the characteristic radioactive "tail" (see, e.g., Sollerman, Cumming, & Lundqvist 1998; Turatto et al. 1998; Benetti et al. 2002). If the hydrogen envelope is gone (Type Ib/c), the consequences for the light curve are more dramatic, and the supernova may be, for practical purposes, invisible.

Four cases of nickel-deficient supernovae may be noted:

1. *Stars in the mass range 9–11 $M_\odot$.*—Such stars have steep density gradients at the edge of degenerate cores. The shock wave from core collapse heats very little material to more than 5×10^9 K and very little ($\lesssim$0.01 $M_\odot$) ^{56}Ni is ejected (Mayle & Wilson 1988).

2. *Stars that make ^{56}Ni but where the ^{56}Ni falls back into the remnant.*—This occurs for more massive stars with the threshold mass dependent on both the presupernova structure and the explosion mechanism and energy. The boundary here is somewhat fuzzy because of the operation of mixing in conjunction with fallback. The lower limit for this regime is probably slightly larger than that for BH formation by fallback; the upper limit is where BHs are formed directly without initiating a supernova, i.e., 10 $M_\odot \lesssim$ helium core mass $\lesssim$ 15 $M_\odot$ (stellar masses 30 $M_\odot \lesssim M \lesssim$ 40 $M_\odot$ without mass loss).

3. *Pair-instability supernovae with helium core masses in the range 65 to $\lesssim$85 $M_\odot$.*—Pair-instability supernovae, which probably only existed in the early universe, can have light curves ranging from very faint, if they have lost their hydrogen envelopes and eject no ^{56}Ni, to exceptionally brilliant, if the converse is true (helium core $\gtrsim$100 $M_\odot$; Heger & Woosley 2002; Heger et al. 2002).

4. *Pulsational pair-instability supernovae with helium core masses in the range $\gtrsim$40–65 $M_\odot$.*—This instability occurs after central carbon burning but before the collapse. Although each pulse can have up to several 10^{51} ergs, only the outer layers of the star are expelled and contain no ^{56}Ni (see below).

4.4. *Pair-Instability Supernovae*

Very massive stars ($M \gtrsim 100\ M_\odot$) still form in the present galaxy (Najarro & Figer 1998; Eikenberry et al. 2001), but above $\approx$60 $M_\odot$, nuclear-powered and opacity-driven pulsations occur that increase the mass loss (ϵ- and κ-mechanisms). Recently, Baraffe et al. (2001) have shown that both mechanisms are suppressed in extreme Population III stars. Therefore, it seems reasonable to assume that at sufficiently low metallicity ($Z \lesssim 10^{-4}\ Z_\odot$) very massive stars may retain most of their mass through the end of central helium burning, forming a massive helium core (Baraffe et al. 2001; Kudritzki 2002; Marigo, Chiosi, & Kudritzki 2003).

For zero-metallicity stars above $\sim$100 $M_\odot$ (helium cores $\gtrsim$42 $M_\odot$; Woosley 1986; Chiosi 2000; Heger & Woosley 2002), stars encounter the pair instability after central carbon burning (see, e.g., Bond, Arnett, & Carr 1984; Heger & Woosley 2002). Between $\sim$100 and $\sim$140 $M_\odot$ (helium core mass $\lesssim$65 $M_\odot$) the instability results in violent pulsations, but not complete disruption. The implosive burning is not energetic enough to explode the star. Depending on the mass of the star and the strength of the initial pulse, subsequent pulses follow after $\lesssim$1 to $\gtrsim$10,000 yr. These pulsations continue until the star has lost so much mass or decreased in central entropy that it no longer encounters the pair instability before forming an iron core in hydrostatic equilibrium. Since the iron core mass is large and the entropy high, such a star probably finally make black holes.

The typical energy of these pulses can reach a few times 10^{51} ergs and easily expels the hydrogen envelope, which is only loosely bound, in the first pulse (Heger & Woosley 2002)—when these stars finally collapse they are thus hydrogen-free. Subsequent pulses may eject the outer layers of the helium core as well. Although the kinetic energy of these pulses may be well in excess of normal supernovae, they are intrinsically less bright since they lack any ^{56}Ni or other radioactivities that could power an extended light curve. However, the collision of shells ejected by multiple pulses could lead to a bright display.

For stars between $\sim$140 and $\sim$260 $M_\odot$ (helium cores of $\sim$64–133 $M_\odot$), the pair instability is violent enough to completely disrupt the star in the first pulse (Ober, El Eid, & Fricke 1983; Bond et al. 1984; Heger & Woosley 2002). Explosion energies range from $\sim 3 \times 10^{52}$ to $\lesssim 10^{53}$ ergs, and the ejected ^{56}Ni mass ranges from 0 to $\gtrsim$50 $M_\odot$ at the high-mass end (Heger & Woosley 2002). Above $\sim$260 $M_\odot$, the stars directly collapse to a black hole (Fryer et al. 2001; Heger & Woosley 2002). Rotation would, of course, affect these mass limits.

4.5. *Very Energetic and Asymmetric Supernovae*

4.5.1. *Jet-powered Supernovae*

A jet-driven supernova (JetSN) is a grossly asymmetric supernova in which most of the energy comes from bipolar outflow from a central object. These JetSNe can be significantly more energetic than "normal" supernovae and are our model for making "*hypernovae*" (Paczynski 1998; Nomoto et al. 2003). Although such supernovae may occur in association with gamma-ray bursts (GRBs), not all jet-powered supernovae will have sufficiently relativistic ejecta to make such a hard display. The class of jet-powered supernovae is thus a broad one, having GRB progenitors as a subset.

Jet-driven supernovae can be formed with or without hydrogen envelopes (MacFadyen, Woosley, & Heger 2001; Nomoto et al. 2003; Fig. 4). The hydrogen-free JetSNe are closely related to GRBs. Whether such stars produce JetSNe or GRBs (or both) depends on the rotation and the explosion mechanism. Until we understand both better, we cannot distinguish between the two.

4.5.2. *Gamma-Ray Bursts and Collapsars*

The currently favored model for the formation of GRBs assumes that a narrowly beamed ($\theta \lesssim 10^\circ$), highly relativistic jet ($\Gamma > 100$) leaves a compact "engine" and produces gamma-rays by either internal shocks or running into some external medium (Frail et al. 2001). Currently two classes of GRBs are distinguished: long and short bursts (Fishman & Meegan 1995). It is assumed that the short class might originate from binary neutron stars (Eichler et al. 1989); the long class could be produced by the collapse of the core of a massive star (see, e.g., Popham, Woosley, & Fryer 1999). In the present work we adopt this assumption, focus on the long class of GRBs, and use "GRB" synonymously for this class.

The term "collapsar" is used to describe all massive stars whose cores collapse to black holes and that have sufficient angular momentum to form a disk. There are three possible varieties (see Table 3):

Type I: Collapsars that form black holes "directly" during the collapse of a massive core.—Although the star collapses and initially forms a proto–neutron star, it is unable to launch a supernova shock and eventually (after $\sim$1 s) collapses to form a black hole (Woosley 1993; MacFadyen & Woosley 1999).

Type II: Collapsars that form black holes by fallback after an initial supernova shock has been launched (*MacFadyen et al. 2001*).—The explosion is too weak to eject much of the star, and the subsequent fallback of material causes the neutron star in the core to collapse and form a black hole.

Type III: Collapsars that do not form proto–neutron stars at all, but instead quickly collapse into massive black holes, which grow through accretion (*Fryer et al. 2001*).—These collapsars lead to the formation of massive ($\sim$300 $M_\odot$) black holes.

The results can be summarized as follows:

1. Type I and II collapsars without a hydrogen envelope can make ordinary GRBs, although those of Type II will tend to be longer.
2. Type II and III collapsars without a hydrogen envelope—maybe even with—can make very long GRBs (in their rest frame).
3. All three types can make bright jet-powered supernovae if a hydrogen envelope is present.

Although we have described them as GRB progenitors, collapsars probably produce a variety of outbursts, from X-ray flashes to jet-driven supernovae. Calculations to reliably show which stars make GRBs as opposed to just black holes are presently lacking (though see Heger & Woosley 2003). Here we will assume that collapsars are made by some subset of those stars that make black holes (Fig. 3).

It is agreed, however, that collapsars can only form GRBs if the star has lost its hydrogen envelope prior to collapse.

TABLE 3
COLLAPSAR VARIETIES

Type	Timescale	Energy Budget	Initial BH Mass
I.....	Short	Low	Small
II.....	Long	Low	Small
III	Long	High	Large

Mass loss depends on both the stellar mass and metallicity, and as both increase, the star uncovers more and more of its hydrogen envelope. The green curve in Figures 3 and 4 denotes the boundary between stars that retain some of their hydrogen envelope and those that lose all of their hydrogen through mass loss. Above $\sim$30 $M_\odot$, mass loss from winds become important, and as the initial mass of the star increases, lower and lower metallicities are required to retain the hydrogen envelope. Between 100 and 140 $M_\odot$, pulsational pair instabilities are able to drive off the hydrogen layers of the star, even at zero metallicities. This boundary, which determines where stars lose their hydrogen envelopes, marks the lower bound for GRB-producing collapsars. The upper bound is set by those stars that collapse to form black holes.

5. STELLAR POPULATIONS

With our evaluation of the possible fates of massive stars from § 4, we estimate the distribution of compact remnants and of observable outbursts produced by these single stars. The results will be uncertain. Not only do the predictions depend sensitively on the regions outlined in Figures 1–4 but also on the initial mass function (IMF) and its evolution.

In Figure 5, we plot the fraction of massive stars forming neutron stars (*solid line*) and black holes (*dotted line*), assuming a Salpeter IMF (Salpeter 1955). At low metallicities, roughly 20% of massive stars form black holes and roughly 75% form neutron stars. Half of those black holes form through fallback and the other half through direct collapse. Only 4% of black holes made form as massive black holes ($>$200 $M_\odot$). Just 1% of massive stars form pair-instability supernovae (leaving behind no remnant whatsoever). As the metallicity increases, the fraction of stars producing black holes first increases slightly (as the pair-instability mechanism is shut off) and then decreases near solar metallicity as most massive stars lose so much mass that they collapse to form neutron stars instead of black holes. At these high metallicities, all black holes are formed through fallback. Note that direct-collapse black holes are larger than fallback black holes and that black holes will be larger, on average, at low metallicity. In addition, if the black hole kick mechanism is powered by the supernova explosion, direct black holes will not receive kicks, and these large black holes will tend to have small spatial velocities.

There is increasing evidence that the IMF is more skewed toward massive stars (relative to a Salpeter IMF) at low metallicities (see, e.g., Bromm et al. 2001; Abel, Bryan, & Norman 2002, 2000). To include these effects, we have used the IMF for Population III by Nakamura & Umemura (2001). The thin lines in Figure 5 show the change in the distribution of black holes and neutron stars using the Nakamura & Umemura (2001) IMF with the following parameters: $m_{p_1} = 1.5$, $m_{p_2} = 50$, $\kappa = 0.5$, and $\alpha = \beta = 1.35$ (see Nakamura & Umemura 2001 for details). We employ this IMF up to a metallicity that corresponds to the last occurrence of (nonpulsational) pair-instability supernovae (Fig. 2). Note that at low metallicities, where the IMF is skewed toward massive stars, the fraction of massive stars that form black holes is nearly twice as large as that predicted by a Salpeter IMF. Most of these black holes are formed through direct collapse.

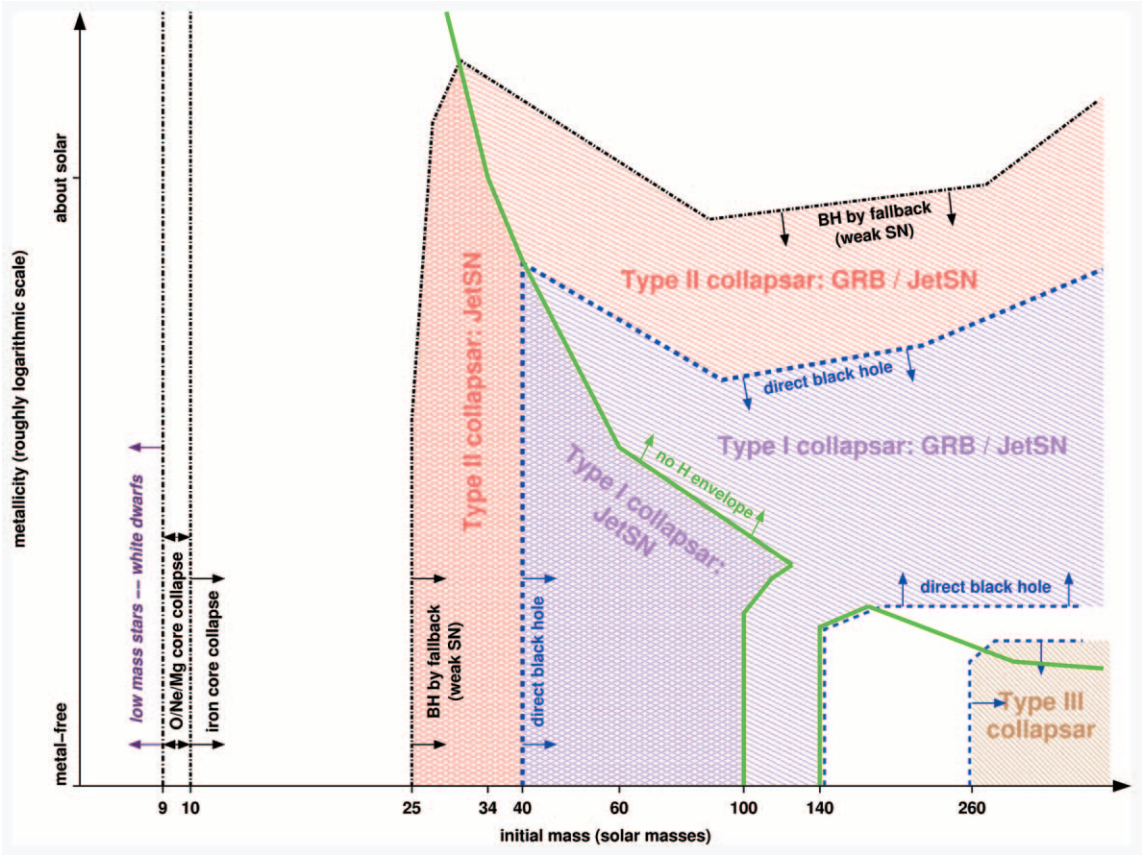

FIG. 3.—Collapsar types resulting from single massive stars as a function of initial metallicity and initial mass. Lines have the same meaning as in Fig. 1. Our main distinction is between collapsars that form from fallback (Type II; *red*) and directly (Type I; *pink*). We subdivide these into those that have a hydrogen envelope (*cross-hatching*), only able to form jet-powered supernovae (JetSNe) and hydrogen-free collapsars (*diagonal cross-hatching*), possibly making either JetSNe or GRBs (see also Fig. 4). The first subclass is located below the thick green line of loss of the hydrogen envelope, and the second is above it. The light brown diagonal hatching at high mass and low metallicity indicates the regime of very massive black holes formed directly (Type III collapsars) that collapse on the pair-instability and photodisintegration. Since the collapsars scenario require the formation of a BH, at low mass (left in the figure) or high metallicity (top of the figure) and in the strip of pair-instability supernovae (lower right) no collapsars occur (*white*).

If the mass limit at which weak supernovae occur decreases from 25 to 20 $M_{\odot}$, the fraction of neutron stars and typical Type IIp supernovae at low metallicities drops below 70%. The fraction of stars that form weak IIp supernovae and black holes increases to compensate for this decrease. Table 4 summarizes the population fractions for different assumptions for the IMF and for the lower limit of the stellar core mass (i.e., lower limit of the initial mass for hydrogen-covered stars), resulting in fallback black hole formation. As mentioned above, here we assume that this corresponds to the maximum stellar/core mass-forming strong SNe.

In Figure 6*a*, we show the distribution of Type II supernovae. Most (~90%) single massive stars produce Type II SNe (*solid line*). Most of these produce normal Type IIp SNe (*dashed line*). Roughly 10% of all massive stars produce weak Type IIp SNe (*dot-dashed line*). As the metallicity approaches solar, some fraction of massive stars will produce Type IIL/b SNe. In Figure 6*b*, we plot the Type Ib/c SNe distribution. Single stars will not produce Type Ib/c SNe until the metallicity gets large enough to drive strong winds. At first, most Type Ib/c SNe will be produced by "weak" explosions that form black holes by fallback (*dot-dashed line*), but as the metallicity rises, an increasing fraction of "strong" Ib/c SNe is produced (*long-dashed line*). Pair-instability SNe only occur at low metallicities, and for our choice of IMF, both pulsational and nonpulsational pair-instability supernovae each constitute only about 1% of all massive stars. When using the IMF by Nakamura & Umemura (2001) the pair SNe rates increase by a factor ~3 (*thin lines*). Note that in Figure 6*b* the pair SNe rate is scaled by a factor of 10.

Figure 7 shows the distribution of GRBs and JetSNe (explosions arising from collapsars). Since in the frame of the present paper we cannot well distinguish between GRBs and JetSNe, and lacking a better understanding of rotation, these rates are upper limits only. The solid line in Figure 7 reflects the total fraction of massive, single stars that could produce GRBs or JetSNe. The dotted line denotes the fraction of massive stars that could produce GRBs. To produce GRBs, the massive star must lose all of its hydrogen envelope but still collapse to form a black hole. Hence, there is a narrow window of metallicities that allow GRB production in single stars. Because pulsational instabilities are able to eject the hydrogen envelope of stars even at zero metallicities, some GRBs could be formed at low metallicities. As in Figure 5, the thin lines denote the differences caused by using the Nakamura & Umemura (2001) IMF at low metallicities.

To determine a distribution of evolutionary outcomes versus redshift, we not only need to know the metallicity dependence of stellar winds, but we also need to know the metal distribution and spread as a function of redshift. This cosmic age-metallicity relation is likely to have large spreads

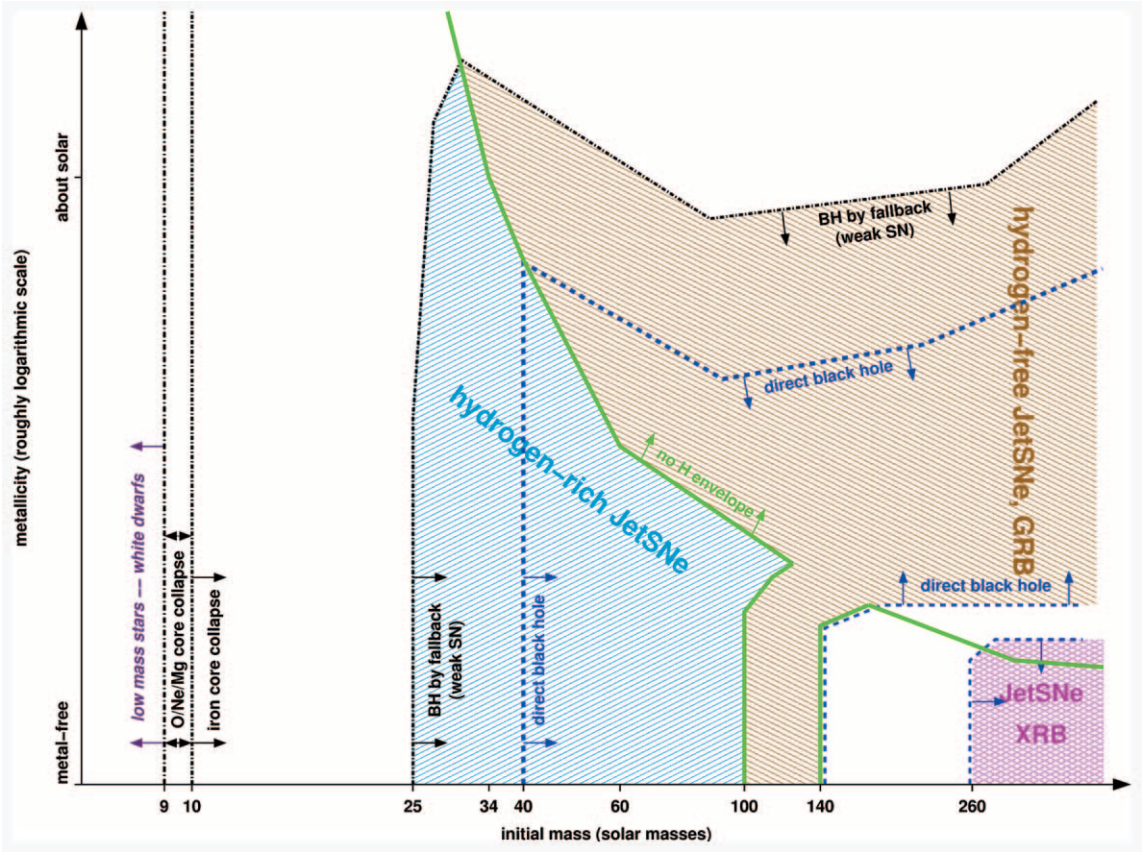

FIG. 4.—Jet-driven supernovae types as a function of initial metallicity and initial mass. Lines have the same meaning as in Fig. 1. The regimes in which hydrogen-rich JetSNe are possible (below the thick green line indicating loss of the hydrogen envelope) is indicated by cyan hatching and that of hydrogen-free JetSNe by light brown hatching (above the thick green line). In the latter regime GRBs may also be possible, while in the first regime a hydrogen envelope is present and the travel time of a relativistic jet though it is much bigger than typical observed GRB durations. In the region of very massive black hole formation (lower right corner; *magenta cross-hatching*) long JetSNe and long X-ray outbursts may occur since the bigger mass scale of these objects also translates into a longer timescale. If these objects are at cosmological distances, additionally the apparent timescale and wavelength of both are stretched.

and a weak trend (Pei & Fall 1995), as is also the case for this relation within the Milky Way (Matteucci 2001; Pagel 1997). These dependencies are difficult to determine because on a more global galactic or cosmological scale metals may be redistributed so that, e.g., most of the metals even for low-metallicity stars could be produced in stars of metallicity. However, to give a flavor of possible redshift effects, we assume that the metallicity axis in Figures 1–4 is indeed logarithmic and use the metallicity redshift distribution assumed by Lloyd-Ronning et al. (2002): Pei, Fall, & Hauser (1999) distribution versus redshift with a Gaussian spread using a 1 σ deviation set to 0.5 in the logarithm of the metallicity. With these assumptions we can determine the distribution of neutron stars (*thick solid line*), black holes (*thick dotted line*), Type II SNe (*thin solid line*), Type Ib/c SNe (*thin dotted line*), and pair supernovae (*thin dashed line*) as a function of redshift (or look-back time; Fig. 8). This suggests a trend in the populations of massive star outcomes versus redshift.

6. UNCERTAINTIES AND POSSIBLE CONSEQUENCES

6.1. *Uncertainties in Mass Loss*

Our mass-loss rates explicitly include only radiatively driven mass loss, although the exact nature of the Wolf-Rayet star mass loss is unknown. We do not include pulsational ejection and similar eruptions by excretion disks in rapidly rotating stars ("Ω-limit"; Langer 1997). The magnitude of these mass-loss mechanisms depends on the composition of the star. For hot stars, both the absolute value and the metallicity dependence of wind-driven mass loss are reasonably well understood and theoretically modeled (Kudritzki 2000, 2002). For most of the other mass-loss mechanisms and temperature and mass regimes, we have insufficient observational data or theoretical mass-loss models to make precise predictions of a massive star's destiny. This is one reason we do not give precise values for metallicity along the axes in Figures 1–4.

Although there is general consensus that reducing the initial metallicity of a massive star will increase its mass when it dies, the scaling of mass loss with Z during different stages of the evolution is controversial. We have made the simplest possible assumption, that mass-loss rates scale everywhere as the square root of initial metallicity, essentially as the square root of the iron abundance. This is almost certainly naive. Vink, de Koter, & Lamers (2001) argue for a scaling $Z^{0.69}$ for stars with $T_{\rm eff} > 25,000$ K and $Z^{0.64}$ for B supergiants with $T_{\rm eff} < 25,000$ K. Nugis & Lamers (2000) argued for a $Z^{0.5}$ scaling in WN and WC stars, but for WC stars at least they had in mind the abundance of carbon in the atmosphere of the star, not the initial metallicity. On theoretical grounds, Kudritzki (2002) discusses a universal scaling for mass loss in hot stars that goes at $Z^{0.5}$ but that has a threshold below which the mass loss declines more sharply.

For red supergiants, even the mass loss at solar metallicity is not well determined. At higher stellar masses the mass loss

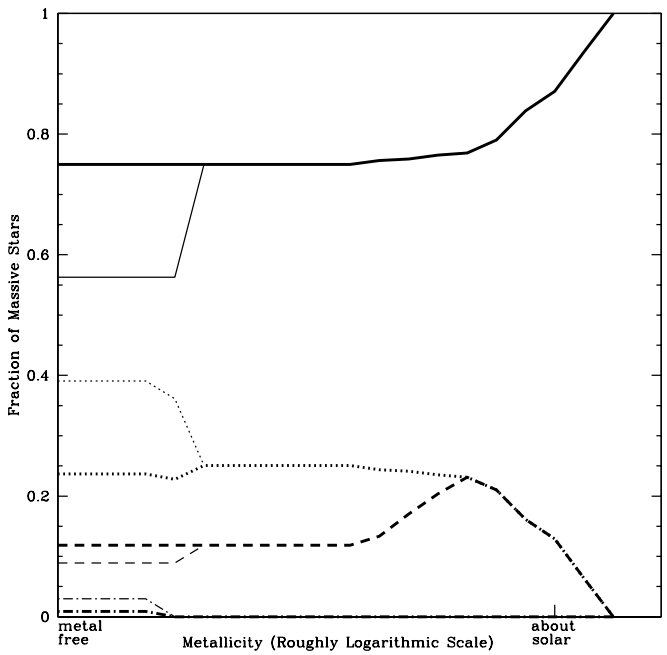

FIG. 5.—Fraction of massive stars that form neutron stars (*solid line*) and black holes (*dotted line*) as a function of metallicity for a Salpeter initial mass function (*thick lines*; Salpeter 1955). The dashed lines denote just those black holes formed through fallback and the dot-dashed lines denote black holes formed from very massive (>300 $M_\odot$) stars. The thin lines arise from assuming the IMF at low metallicities is given by Nakamura & Umemura (2001) at low metallicity (see § 5). Note that at low metallicities, pair-instability supernovae leave no compact remnant whatsoever, so that in this regime the total of all fractions is less than 1.

from luminous blue variables and WR stars also constitutes a major source of uncertainty, as do pulsationally induced and rotationally induced outflows (see above).

6.2. *Uncertainty in the Explosion Mechanism*

The mechanism whereby the collapse of the iron core in a massive star results in a strong explosion has been debated for decades. The current paradigm is based on a neutrino-powered "hot bubble" formed just outside the young proto–neutron star (Herant et al. 1994; Burrows, Hayes, & Fryxell 1995; Janka & Mueller 1996), but even the validity of this paradigm is debated along with its specific predictions (Mezzacappa et al. 1998) and has not been resolved by recent multidimensional calculations (Janka et al. 2003). The role of rotation and magnetic fields is also contentious (Leblanc & Wilson 1970; Fryer & Heger 2000; Ardeljan, Bisnovatyi-Kogan, & Moiseenko 2001; Wheeler, Meier, & Wilson 2002; § 6.3).

Our intuition here has been guided by parametric surveys in which the explosion is simulated using a piston. The numerous uncertainties are thus mapped into choices of the piston's location and motion. These parameters are constrained by the requirement that the explosion not eject too much neutron-rich material (hence a minimum mass interior to the piston) and that the kinetic energy of the explosion measured at infinity be 10^{51} ergs, although a single event, SN 1987A, occurred for a representative helium core mass (6 $M_\odot$) and had a measured kinetic energy at infinity of $\sim(1\text{–}1.5) \times 10^{51}$ ergs (Woosley 1988; Arnett et al. 1989; Bethe & Pizzochero 1990). The requirement that supernovae typically make $\sim$0.1 $M_\odot$ of ^{56}Ni also means that the piston cannot be situated too far out or produce too weak an explosion. There are also more subtle conditions—that the

TABLE 4
REMNANT AND SUPERNOVA POPULATION YIELDS FOR DIFFERENT METALLICITIES, IMFS, AND MASS LIMITS

	Zero Metallicity				Solar Metallicity	
	High $M_{\rm FBH}^{\rm lim}$		Low $M_{\rm FBH}^{\rm lim}$		High $M_{\rm FBH}^{\rm lim}$	Low $M_{\rm FBH}^{\rm lim}$
Object	$\rm IMF_{Sal}$	$\rm IMF_{NU}$	$\rm IMF_{Sal}$	$\rm IMF_{NU}$	$\rm IMF_{Sal}$	$\rm IMF_{Sal}$
Remnants						
NS	75	56	66	50	87	75
BH	23	36	32	43	13	25
MBH	0.9	3.0	0.9	3.0	0	0
Supernovae						
IIp strong	75	56	66	50	77	70
IIp weak	12	8.9	21	16	0	6.9
IIL/b	0	0	0	0	6.4	6.4
Ib/c strong	0	0	0	0	9.2	5.1
Ib/c weak	0	0	0	0	7.6	12
Other Outbursts						
Pulsar pair	1.4	4.7	1.4	4.7	0	0
Pair SNe	1.4	4.6	1.4	4.6	0	0
Jet SNe	24	39	33	46	13	25
GRBs	1.4	3.4	1.4	4.7	7.8	12

NOTE.—For solar metallicity, we use the IMF by Salpeter 1955 ($\rm IMF_{Sal}$); for zero metallicity, we additionally supply the results for the IMF by Nakamura & Umemura 2001 ($\rm IMF_{NU}$). We give the results for two different lower mass limits for fall-back black hole formation ($M_{\rm FBH}^{\rm lim}$): *high* corresponds to 25 $M_\odot$ and *low* to 20 $M_\odot$ (Fryer 1999).

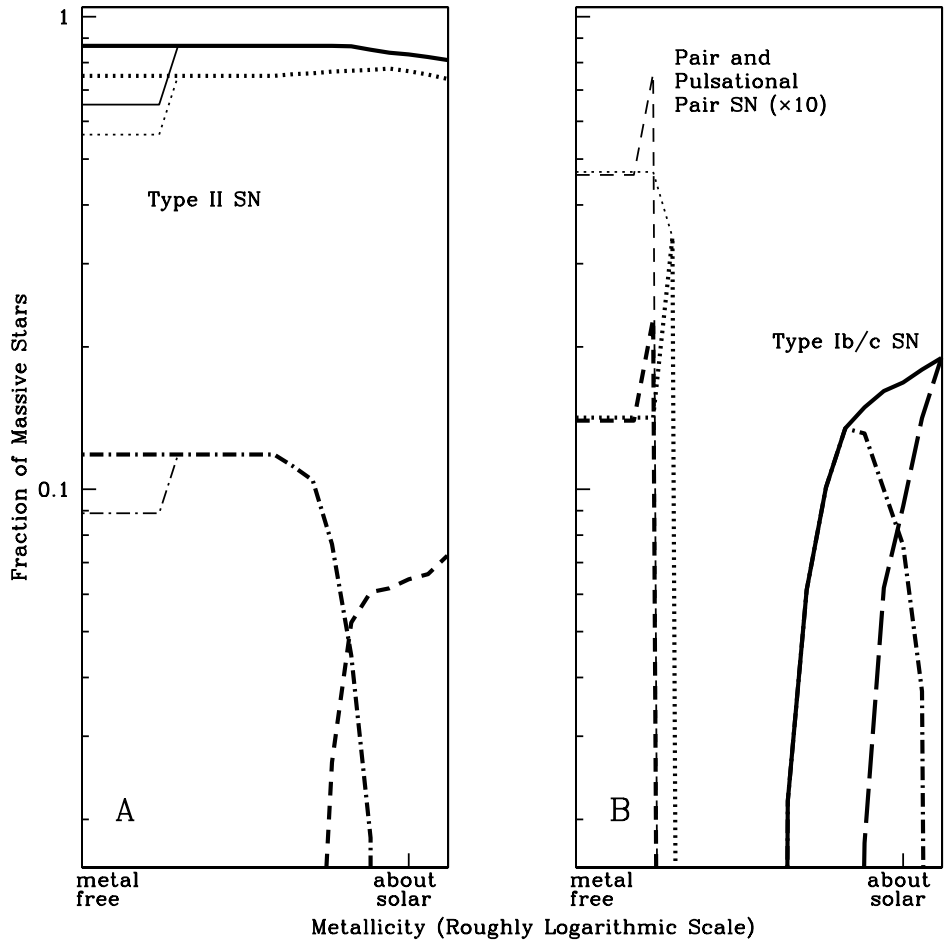

FIG. 6.—Fraction of massive stars that form supernovae for a Salpeter initial mass function (*thick lines*; Salpeter 1955). At low redshifts we use an alternate initial mass function (*thin lines*) from Nakamura & Umemura (2001). Most single stars become (*a*) Type II supernovae (*solid line*), and most of these are strong IIp SNe (*dotted line*). Roughly 15 % of Type II SNe are weak Type IIp supernovae (*dot-dashed line*). As the metallicity approaches solar, the fraction of weak supernovae decreases and a small fraction of Type IIL/b SNe are produced (*dashed line*). (*b*) Type Ib/c supernovae are not produced until the metallicity approaches solar (*solid line*), and most of these SNe will be weak (*dot-dashed line*). Not until the metallicity exceeds solar are strong Ib/c SNe produced (*long-dashed line*). Pair-instability supernovae (*dashed line*) and pulsational pair-instability supernovae (*dotted line*) are rare and only produced at low metallicities. Their fraction depends strongly on the unknown IMF at these low metallicities. Note that in the figure we multiply the pair-instability SNe fraction by a factor 10.

mass cut frequently occurs in a location where past (successful) calculations of the explosion have found it, that the distribution of remnant masses resemble what is observed for neutron stars, that the integrated ensemble of abundances resemble Population I in our galaxy, and so on.

Figure 9 shows the remnant masses for a survey of explosions in solar metallicity stars that neglects mass loss. The progenitor stars described in Woosley et al. (2002) were exploded using a piston located at the edge of the "iron core." The iron core was defined by the location of an abrupt jump in the neutron excess (electron mole number $= Y_e = 0.49$). A constant kinetic energy at infinity (1.2×10^{51} ergs) was assumed (see also Woosley & Weaver 1995). In fact, the explosion energy will probably vary with mass. Fryer (1999) calculates that the explosion energy will actually weaken as the mass of the helium core increases. Thus, fallback could have an even earlier onset and more dramatic effects than Figure 9 would suggest.

The apparent nonmonotonic behavior in Figure 9 is largely a consequence of the choice of where the piston was sited. The neutronized iron core may have a variable mass that depends on details of oxygen and silicon shell burning (Woosley et al. 2002). The density gradient around that core can also be highly variable. Thus, enforcing a constant kinetic energy at infinity does not always lead to a predictable variation of remnant mass with initial mass. More recent unpublished calculations by A. Heger et al. (2003, in preparation), also of zero-metallicity stars, place the piston at an entropy jump (dimensionless entropy $S/N_A k_B = 4$) rather than a Y_e jump. This choice, which is more consistent with explosion models, assumes that an explosion develops when the accretion rate declines rapidly. The rapid decline is associated with the density (and entropy) discontinuity near the base of the oxygen-burning shell. Preliminary results seem to give more monotonic results. In particular, the bump around 17 $M_\odot$ in Figure 9 is absent, but that around 25 $M_\odot$ was still present. However, this result also depends on the explosion energy assumed.

Nevertheless, Figure 9 does suggest that the lines separating black hole formation by fallback from neutron stars in Figures 1–4 should be interpreted only as indicating trends. They may not be as smooth or as monotonic as indicated.

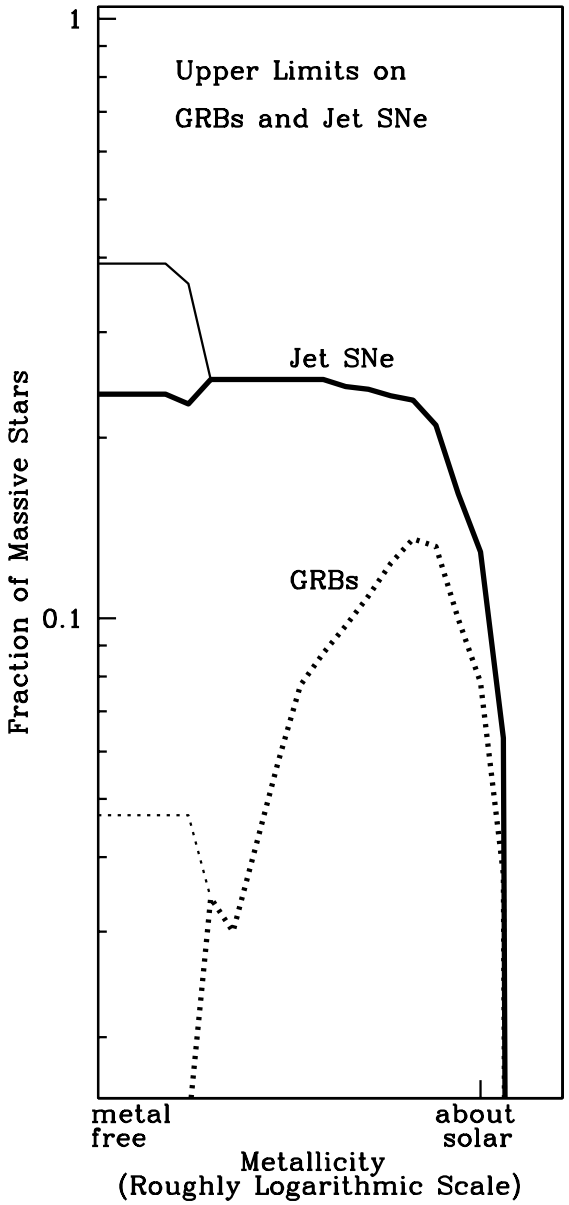

FIG. 7.—Upper limits on the fraction of massive single stars that form jet-driven supernovae and gamma-ray bursts for a Salpeter initial mass function (*thick lines*; Salpeter 1955). At low redshifts we use an alternate initial mass function (*thin lines*) from Nakamura & Umemura (2001). These upper limits are determined assuming that all massive stars have the necessary rotation rates to produce collapsars. Single stars produce GRBs mostly in a narrow range of metallicities but can produce Jet SNe at all metallicities until the metallicity is so high that mass loss prohibits the formation of black holes.

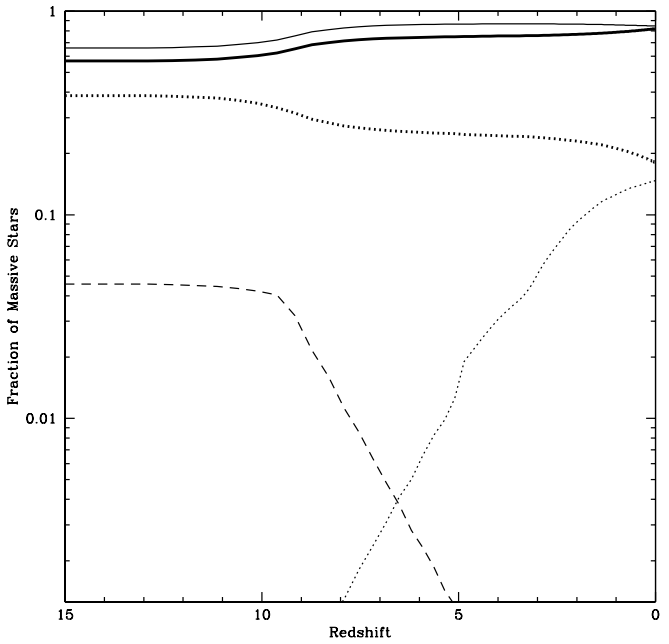

FIG. 8.—Distribution of neutron stars (*thick solid line*), black holes (*thick dotted line*), Type II SNe (*thin solid line*), Type Ib/c SNe (*thin dotted line*), and pair supernovae (*thin dashed line*) as a function of redshift. We have assumed that the metallicity axis in Figs. 1 and 2 is indeed logarithmic with the maximum mass for which pair creation supernovae occur (Fig. 2), corresponding to a metallicity of 10^{-4} solar. We have used the metallicity redshift distribution assumed by Lloyd-Ronning et al. (2002): Pei et al. (1999) distribution vs. redshift with a Gaussian spread using a 1 σ deviation set to 0.5 in the logarithm of the metallicity. This gives an idea of the trends in the populations of massive single star outcomes as a function of redshift. Given the various assumptions that have to be made for this type of analysis, the resulting absolute numbers should be interpreted with a great caution.

6.3. *Uncertainty in the Effects of Rotation*

Rotation can enhance the mass loss in stars, and a spread in initial rotation can smear out the transitions between the different mass and metallicity regimes. We have not considered cases in which rotationally enhanced mass loss might be important. In such cases the limiting mass for loss of the hydrogen envelope could be lowered and, at the same time, the mass of the helium core increased (Heger, Langer, & Woosley 2000; Meynet & Maeder 2000). The higher mass loss would tend to lower the metallicity for divisions between Type II and Type Ib/c supernovae as well as the divisions between strong, weak, and no supernova explosions. The higher helium core masses increase the metallicity divisions between strong, weak, and no supernova explosions. The total change will depend on the competition of the larger helium core masses and enhanced mass-loss rate.

If the core is rotating rapidly at collapse, rotation may also influence the explosion mechanism and especially the possibility of making a GRB. Also, pair creation supernovae could be significantly affected by rotation, in particular the lower mass limit for direct black hole formation (Glatzel, Fricke, & El Eid 1985; Stringfellow & Woosley 1988). Early calculations that followed angular momentum in massive stars (see, e.g., Kippenhahn & Thomas 1970; Kippenhahn, Meyer-Hofmeister, & Thomas 1970; Endal & Sofia 1976, 1978; Tassoul 2000) all found sufficient angular momentum retained in the core to reach critical rotation ("breakup velocity") before the final central burning phases. More recent calculations by Heger (1998) and Heger et al. (2000) find presupernova core rotation rates in massive stars that would lead to submillisecond neutrons stars just around break up if angular momentum were conserved perfectly during the collapse. Calculations by Meynet & Maeder (1997), Maeder & Zahn (1998), and A. Maeder & G. Meynet (2000, private communication) indicate core rotation rates after central helium burning similar to those found by Heger et al. (2000).

Recently, Spruit (2002) has discussed a "dynamo" mechanism based on the interchange instability that allows the

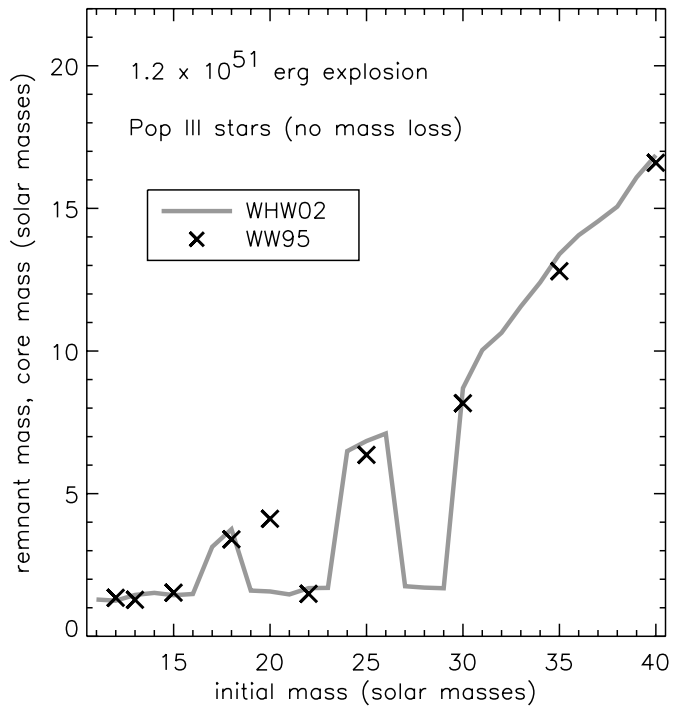

FIG. 9.—Remnant masses of metal-free stars as a function of initial mass for stars from Woosley et al. (2002; WHW02, *solid line*) assuming a constant kinetic energy of the ejecta of 1.2×10^{51} ergs. The explosions were simulated by a piston at the edge of the deleptonized core similar to Woosley & Weaver (1995; WW95, *crosses*).

estimation of magnetic torques to be included in models for stellar evolution. Preliminary calculations by Heger et al. (2003) and A. Heger et al. (2003, in preparation) that include these torques find a presupernova angular momentum equivalent to 5–10 ms—still somewhat faster than that observed in young pulsars, but too slow for collapsars. If the estimates of magnetic torques by Spruit (2002) are valid, then single stars are unlikely to produce collapsars and rotation is probably not a factor in the explosion of common supernovae. Nevertheless, in Figure 3 we indicate the regimes where the structure of the star, excluding the question of sufficient rotation, is favorable for collapsars and GRBs.

7. CONCLUSIONS AND OBSERVATIONAL TESTS

We have described, qualitatively, the likely fates of single massive stars as a function of metallicity. Our results suggest various trends in the observations of these objects that may be subject to observational tests.

1. Normal Type Ib/c SNe are not produced by single stars until the metallicity is well above solar. Otherwise the helium core mass at death is too large. This implies that most Type Ib/c SNe are produced in binary systems where the binary companion aids in removing the hydrogen envelope of the collapsing star.

2. Although less extreme than Type Ib/c SNe, single stars also do not produce Type IIL/b SNe at low metallicities. Similar to Type Ib/c SNe, Type IIL/b SNe from single stars are probably "weak" SNe until the metallicity exceeds solar, also implying that Type IIL/b SNe are produced in binaries.

3. If GRBs are produced by single-star collapse (perhaps unlikely given the constraints on angular momentum), single stars only make up a small subset of GRB progenitors at higher metallicities. It is more likely that binary systems form GRBs. Such systems will occur more frequently at low metallicities (Fryer, Woosley, & Hartmann 1999).

4. Jet-driven supernovae from single stars are likely to be much more common than GRBs from single stars.

It is difficult to make direct comparisons to observations without including binary stars in our analysis. Observations tell us that for S0a–Sb galaxies, the ratio of Type II supernovae over Type Ib/c supernovae is between 1.2 and 12. For Sbc–Sd galaxies, this ratio is between 2.1 and 16 (Cappelaro et al. 1997). At solar metallicity, we predict this ratio to be 5. However, with a slight decrease in metallicity, our basic picture would predict essentially no Type Ib/c supernovae. But at these lower metallicities, binary stars will dominate the type Ib/c event rate, and even at solar metallicities, the effect of binary stars may well reduce our ratio to the lower limit found in the observations.

We do have a number of results that can place much more firm constraints. First, an increasing number of JetSNe and weak supernovae explosions are being discovered (Nakamura et al. 2001; Sollerman et al. 1998; Turatto et al. 1998). Although there is an observational bias against the discovery of weak supernovae and they are much dimmer than JetSNe, they may still dominate the sample of stars more massive than 25 $M_{\odot}$. Clearly, good statistics (and correct analysis of the systematics) are necessary to determine the relative ratio of jet-driven and weak SNe. With such statistics, we may be able to place constraints on the rotation of massive stellar cores.

If the IMF becomes more top-heavy at low metallicity ($\lesssim 10^{-4}\ Z_{\odot}$; Bromm et al. 2001; Schneider et al. 2002), the number of core-collapse supernovae (mostly Type IIp) and GRBs (if occurring in single stars) should significantly increase at high redshift. If the current estimates of a characteristic mass of $\sim$100 $M_{\odot}$ for primordial stars (Bromm, Coppi, & Larson 1999; Abel et al. 2002; Nakamura & Umemura 2001) is correct, we should expect a large fraction of pair SNe and very massive black holes (or Type III collapsars) at zero metallicity, as well as an increase of massive black holes from stars in the 60–140 $M_{\odot}$ region.

We thank Bruno Leibundgut for discussions about supernova classifications and Thomas Janka, Ewald Müller, and Wolfgang Hillebrandt for many helpful conversations regarding the explosion mechanism. This research has been supported by the NSF (AST 02-06111), the SciDAC Program of the DOE (DE-FC02-01ER41176), the DOE ASCI Program (B347885), and NASA (NAGW-12036). A. H. is supported in part by the Department of Energy under grant B341495 to the Center for Astrophysical Thermonuclear Flashes at the University of Chicago and acknowledges supported by a Fermi Fellowship of the Enrico Fermi Institute at the University of Chicago. The work of C. L. F. was funded by a Feynman Fellowship at LANL.

REFERENCES

Abel, T., Bryan, G. L., & Norman, M. L. 2000, ApJ, 540, 39
———. 2002, Science, 295, 93
Ardeljan, N. V., Bisnovatyi-Kogan, G. S., & Moiseenko, S. G. 2001, Ap&SS Suppl., 276, 295
Arnett, W. D., Bahcall, J. N., Kirshner, R. P., & Woosley, S. E. 1989, ARA&A, 27, 629
Baade, W., & Zwicky, F. 1934, Phys. Rev., 45, 138
Baraffe, I., Heger, A., & Woosley, S. E. 2001, ApJ, 550, 890
Barbon, R., Ciatti, F., & Rosino, L. 1979, A&A, 72, 287
Barkat, Z., Reiss, Y., & Rakavy, G. 1974, ApJ, 193, L21
Benetti, S., Branch, D., Turatto, M., Cappellaro, E., Baron, E., Zampieri, L., Della Valle, M., & Pastorello, A. 2002, MNRAS, 336, 91
Bethe, H. A., & Pizzochero, P. 1990, ApJ, 350, L33
Bond, J. R., Arnett, W. D., & Carr, B. J. 1984, ApJ, 280, 825
Bromm, V., Coppi, P. S., & Larson, R. B. 1999, ApJ, 527, L5
Bromm, V., Ferrara, A., Coppi, P. S., & Larson, R. B. 2001, MNRAS, 328, 969
Brown, G. E., Heger, A., Langer, N., Lee, C.-H., Wellstein, S., & Bethe, H. A. 2001, NewA, 6, 457
Brown, H. 1997, Ph.D. thesis, Ludwig-Maximilians Univ. Munich
Burrows, A., Hayes, J., & Fryxell, B. A. 1995, ApJ, 450, 830
Cappelaro, E., Turatto, M., Tsvetkov, D. Y., Bartunov, O. S., Pollas, C., Evans, R., & Hamuy, M. 1997, A&A, 322, 431
Cassisi, S., & Castellani, V. 1993, ApJS, 88, 509
Chiosi, C. 2000, in The First Stars, ed. A. Weiss, T. G. Abel & V. Hill (Berlin: Springer), 95
Eichler, D., Livio, M., Piran, T., & Schramm, D. N. 1989, Nature, 340, 126
Eikenberry, S. S., et al. 2001, BAAS, 199, 96.05
Endal, A. S., & Sofia, S. 1976, ApJ, 210, 184
———. 1978, ApJ, 220, 279
Ensman, L. M., & Woosley, S. E. 1988, ApJ, 333, 754
Filippenko, A. V. 1997, ARA&A, 35, 309
Fishman, G. J., & Meegan, C. A. 1995, ARA&A, 33, 415
Frail, D. A., et al. 2001, ApJ, 562, L55
Fryer, C. L. 1999, ApJ, 522, 413
Fryer, C. L., & Heger, A. 2000, ApJ, 541, 1033
Fryer, C. L., & Kalogera, V. 2001, ApJ, 554, 548
Fryer, C. L., Woosley, S. E., & Hartmann, D. H. 1999, ApJ, 526, 152
Fryer, C. L., Woosley, S. E., & Heger, A. 2001, ApJ, 550, 372
Garcia-Berro, E., & Iben, I. 1994, ApJ, 434, 306
Garcia-Berro, E., Ritossa, C., & Iben, I. J. 1997, ApJ, 485, 765
Gaskell, C. M. 1992, ApJ, 389, L17
Glatzel, W., Fricke, K. J., & El Eid, M. F. 1985, A&A, 149, 413
Habets, G. M. H. J. 1986, A&A, 167, 61
Hamann, W.-R., & Koesterke, L. 1998, A&A, 335, 1003
Hamann, W.-R., Koesterke, L., & Wessolowski, U. 1995, A&A, 299, 151
Heger, A. 1998, Ph. D. thesis, Technische Univ. Munich
Heger, A., Langer, N., & Woosley, S. E. 2000, ApJ, 528, 368
Heger, A., & Woosley, S. E. 2002, ApJ, 567, 532
———. 2003, in Woods Hole GRB Conference, ed. R. Vanderspek, in press
Heger, A., Woosley, S. E., Baraffe, I., & Abel, T. 2002, in Lighthouses of the Universe: The Most Luminous Celestial Objects and Their Use for Cosmology, ed. M. Gilfanov, R. A. Siunyaev, & E. Curazov (Berlin: Springer), 369
Heger, A., Woosley, S. E., & Langer, N. 2003, in IAU Symp. 212, A Massive Star Odyssey, from Main Sequence to Supernova, ed. K. A. van der Hucht, A. Herrero, & C. Esteban (San Francisco: ASP), in press
Herant, M., Benz, W., Hix, W. R., Fryer, C. L., & Colgate, S. A. 1994, ApJ, 435, 339
Iben, I. J., Ritossa, C., & Garcia-Berro, E. 1997, ApJ, 489, 772
Janka, H.-T., Buras, R., Kifonidis, K., Rampp, M., & Plewa, T. 2003, in Core Collapse of Massive Stars, ed. C. L. Fryer (Dordrecht: Kluwer), in press
Janka, H.-T., & Mueller, E. 1996, A&A, 306, 167
Kippenhahn, R., Meyer-Hofmeister, E., & Thomas, H. C. 1970, A&A, 5, 155
Kippenhahn, R., & Thomas, H.-C. 1970, in IAU Colloq. 4, Stellar Rotation, ed. A. Slettebak (New York: Gordon & Breach), 20
Kudritzki, R. 2000, in The First Stars, ed. A. Weiss, T. G. Abel, & V. Hill (Berlin: Springer), 127
Kudritzki, R. P. 2002, ApJ, 577, 389
Langer, N. 1989, A&A, 220, 135
———. 1997, in ASP Conf. Ser. 120, Luminous Blue Variables: Massive Stars in Transition, ed. A. Notta & H. J. G. L. M. Lamers (San Francisco: ASP), 83
Langer, N., & Maeder, A. 1995, A&A, 295, 685
Leblanc, J. M., & Wilson, J. R. 1970, ApJ, 161, 541
Lloyd-Ronning, N. M., Fryer, C. L., & Ramirez-Ruiz, E. 2002, ApJ, 574, 554
MacFadyen, A. I., & Woosley, S. E. 1999, ApJ, 524, 262
MacFadyen, A. I., Woosley, S. E., & Heger, A. 2001, ApJ, 550, 410
Maeder, A., & Zahn, J. 1998, A&A, 334, 1000
Marigo, P., Bressan, A., & Chiosi, C. 1996, A&A, 313, 545
Marigo, P., Chiosi, C., & Kudritzki, R.-P. 2003, A&A, 399, 617
Matteucci, F. 2001, in ASP Conf. Ser. 230, Galaxy Disks and Disk Galaxies, ed. J. Funes & E. Corsini (San Francisco: ASP), 337
Mayle, R., & Wilson, J. R. 1988, ApJ, 334, 909
Meynet, G., & Maeder, A. 1997, A&A, 321, 465
———. 2000, A&A, 361, 101
Mezzacappa, A., Calder, A. C., Bruenn, S. W., Blondin, J. M., Guidry, M. W., Strayer, M. R., & Umar, A. S. 1998, ApJ, 495, 911
Miyaji, S., & Nomoto, K. 1987, ApJ, 318, 307
Miyaji, S., Nomoto, K., Yokoi, K., & Sugimoto, D. 1980, PASJ, 32, 303
Najarro, F., & Figer, D. F. 1998, Ap&SS, 263, 251
Nakamura, F., & Umemura, M. 2001, ApJ, 548, 19
Nakamura, T., Umeda, H., Iwamoto, K., Nomoto, K., Hashimoto, M., Hix, W. R., & Thielemann, F. 2001, ApJ, 555, 880
Nieuwenhuijzen, H., & de Jager, C. 1990, A&A, 231, 134
Nomoto, K. 1984, ApJ, 277, 791
———. 1987, ApJ, 322, 206
Nomoto, K., & Hashimoto, M. 1988, Phys. Rep., 163, 13
Nomoto, K., et al. 2003, in IAU Symp. 212, A Massive Star Odyssey, from Main Sequence to Supernova, ed. K. A. van der Hucht, A. Herrero, & C. Esteban (San Francisco: ASP), in press
Nugis, T., & Lamers, H. J. G. L. M. 2000, A&A, 360, 227
Ober, W. W., El Eid, M. F., & Fricke, K. J. 1983, A&A, 119, 61
Paczynski, B. 1998, ApJ, 494, L45
Pagel, B. E. J. 1997, Nucleosynthesis and Chemical Evolution of Galaxies (Cambridge: Cambridge Univ. Press)
Pei, Y. C., & Fall, S. M. 1995, ApJ, 454, 69
Pei, Y. C., Fall, S. M., & Hauser, M. G. 1999, ApJ, 522, 604
Popham, R., Woosley, S. E., & Fryer, C. 1999, ApJ, 518, 356
Popov, D. V. 1993, ApJ, 414, 712
Ritossa, C., Garcia-Berro, E., & Iben, I. J. 1996, ApJ, 460, 489
———. 1999, ApJ, 515, 381
Salpeter, E. E. 1955, ApJ, 121, 161
Schneider, R., Ferrara, A., Natarajan, P., & Omukai, K. 2002, ApJ, 571, 30
Sollerman, J., Cumming, R. J., & Lundqvist, P. 1998, ApJ, 493, 933
Spruit, H. C. 2002, A&A, 381, 923
Stringfellow, G. S., & Woosley, S. E. 1988, in The Origin and Distribution of the Elements, ed. G. J. Mathews (Singapore: World Scientific), 467
Swartz, D. A., Wheeler, J. C., & Harkness, R. P. 1991, ApJ, 374, 266
Tassoul, J.-L. 2000, Stellar Rotation (Cambridge: Cambridge Univ. Press)
Turatto, M., et al. 1998, ApJ, 498, L129
Vanbeveren, D. 2001, in The Influence of Binaries on Stellar Population Studies, ed. D. Vanbeveren (Dordrecht: Kluwer), 241
Vink, J. S., de Koter, A., & Lamers, H. J. G. L. M. 2001, A&A, 369, 574
Wellstein, S., & Langer, N. 1999, A&A, 350, 148
Wheeler, J. C., Meier, D. L., & Wilson, J. R. 2002, ApJ, 568, 807
Woosley, S. E. 1986, in Nucleosynthesis and Chemical Evolution, ed. B. Hauck, A. Maeder, & G. Meynet (Sauverny: Geneva Obs.), 1
———. 1988, ApJ, 330, 218
———. 1993, ApJ, 405, 273
Woosley, S. E., Heger, A., & Weaver, T. A. 2002, Rev. Mod. Phys., 74, 1015
Woosley, S. E., & Weaver, T. A. 1995, ApJS, 101, 181